The Crustacean Society

OXFORD

Characterization of the complete mitochondrial genome of the striped soldier shrimp, *Plesionika edwardsii* (Brandt, 1851) (Crustacea: Decapoda: Pandalidae), and comparison with other species of Caridea

Claudio A. Jimenez-Ruiz, Francisca Robles, Rafael Navajas-Pérez, Carmelo Ruiz-Rejón and Roberto de la Herrán

Departamento de Genética, Facultad de Ciencias, Universidad de Granada, Granada, 18071, Spain

Correspondence: R. de la Herrán; e-mail: rherran@ugr.es

ABSTRACT

The striped soldier shrimp, *Plesionika edwardsii* (Brandt, 1851) is a pandalid with economic value in the Mediterranean region. We have sequenced and assembled its complete mitochondrial genome, which is 15,956 bp in length and contains the same 37 genes found in most metazoan mitochondrial genomes. Its gene order and nucleotide content are similar to most of the caridean mitochondrial genomes. In the comparative analysis, however, we detected in other species changes in the gene order that could be mediated by the recombination of transfer RNA genes, as well as AT skew shifts that could indicate changes in the origins of replication. All protein-coding genes of the mitochondrial genome of *P. edwardsii* seem to be under purifying selection, although the differences in Ka:Ks ratios suggest a disparity in the mutational constraints of some genes. This genome also presents a 1,118 bp-long non-coding sequence that encompass the control region. We have been able to find a previously described conserved sequence block in this region and assess that it forms a stem-loop structure in different species of Pandalidae, which is a shared feature with the conserved sequence blocks described in the family Alvinocarididae. We also detected microsatellites in the control region of *P. edwardsii* and in other species of Pandalidae and minisatellites in *Lysmata vittata* (Stimpson, 1860) that can account for around 20% of the additional non-coding region of this species. The phylogenetic relationships of *P. edwardsii* with other pandalids were assessed by two analyses: one based on the complete mitochondrial sequences and another based only on the protein-coding genes. Our study, thus, contributes to the genomic resources available for *P. edwardsii* and expands the current biological knowledge about the mitochondrial genomes of other caridean species.

KEY WORDS: Crustacea, mitogenome, mitogenome assembly, phylogenetics, synteny

INTRODUCTION

The mitochondrial genome (mitogenome) of animals is formed by a single circular DNA duplex of typically ~16 kb in size. It includes the same set of 37 genes in most cases: 13 protein-coding genes (PCGs), 22 transfer RNAs (tRNAs), and two ribosomal RNAs (rRNAs), as well as a control region (CR) (Boore, 1999). Mitogenomes are of great interest for studying phylogenetic relationships due to the conservation of its genes, the lack or low level of recombination (Elson & Lightowlers, 2006), a higher evolutionary rate than the nuclear genome, and regions with different rates of evolution. Furthermore, they present genome-level features that can be useful when comparing different species, such as gene order and gene rearrangements, and

repeated and non-coding sequences. (Boore, 1999; Curole & Kocher, 1999; Gissi *et al.*, 2008).

Decapod crustaceans (crabs, crayfishes, lobsters, and shrimps) include many species of commercial importance. The infraorder Caridea is the second largest taxon within the order Decapoda, accounting for over 3,400 species and 36 families (De Grave & Fransen, 2011; Liao *et al.*, 2017). The shrimps of this infraorder populate all aquatic habitats, from deep sea to fresh waters, which makes them of key importance for evolutionary biology (Sun *et al.*, 2020). The genomic resources available for this infraorder, however, are still scarce and particularly the number of complete mitogenomes is limited (Sun *et al.*, 2020). Only 105 different caridean species with their mitogenome are available in

the Genbank database to date. Furthermore, the distribution of these data between families is imbalanced, with the family Atyidae accounting for 26 of these species, 19 species of the family Palaemonidae, 16 Apleidae species, 12 Alvinocarididae species, 10 Hippolytidae species, 10 Pandalidae species, and 12 species of other 6 families. The genus *Plesionika* (Bate, 1888) stands out as the largest in Pandalidae, comprising 93 species, primarily deep-sea shrimps that mainly populate tropical and subtropical waters (Ahamed *et al.*, 2017). *Plesionika sindoi* (Rathbun, 1906) is currently the only species of the genus with a complete mitogenome available in the GenBank database (MH714453). The mitochondrial DNA markers COI and 16S rRNA had been used to establish the phylogenetic relationships between the species of this genus (Silva *et al.*, 2013; Chakraborty *et al.*, 2015; Chakraborty & Kuberan, 2021). These markers have been useful to determine that *Plesionika* may not be monophyletic, as some shallow-water species seem to be paraphyletic to the deep-water species (Silva *et al.*, 2013). A wider availability of complete mitogenomes could help decipher the phylogeny of *Plesionika* by providing multiple loci with different evolution rates.

The soldier striped shrimp *Plesionika edwardsii* (Brandt, 1851) is a cosmopolitan species found in temperate waters between 50 and 680 m of depth (Chan & Yu, 1991), more commonly between 200 and 400 m (Abelló *et al.*, 1988; Chan & Yu, 1991; Fanelli & Cartes, 2004; Santos *et al.*, 2021). The carapace length in this species ranges 7.06–33.28 mm, with females generally larger than males (García-Rodríguez *et al.*, 2000; González *et al.*, 2016; Triay-Portella *et al.*, 2017; Santos *et al.*, 2021). *Plesionika edwardsii* feeds on euphausiids, polychaetes, and mesopelagic fishes (Fanelli & Cartes, 2004). It has a broad reproductive period as ovigerous females can be found throughout the year and can spawn multiple times during the reproductive season (Colloca, 2002; Triay-Portella *et al.*, 2017). Some authors point to a peak in the presence of ovigerous females, but the time of the year of this peak seems to change depending on the location (Martins & Hargreaves, 1991; Santana *et al.*, 1997; García-Rodríguez *et al.*, 2000; Colloca, 2002; González *et al.*, 2016;). *Plesionika edwardsii* is included in the FAO catalogue of species of interest to fisheries (Holthuis, 1980), and its fishing is common along Mediterranean coasts (Holthuis, 1980; González *et al.*, 1992). Despite its economic value, however, this species is still lacking on genomic resources that could help establish the health of its populations and increase our knowledge about its life history.

The aim of our study is to describe the mitogenome of *P edwardsii* and conduct a comparative study between this genome and the previously published mitogenomes of caridean shrimps. We assembled the mitogenome from a sequencing of the total genomic DNA, annotated it, and compared its gene order with the published data of other caridean species. We examined its base composition and the features of its PCGs, as well as the selective constraints of these genes. The characteristics of the non-coding RNA genes were also studied and we analysed the sequence conservation and secondary structure of the control region of this and other pandalid species. We also established the phylogenetic position of *P. edwardsii* in relation to previously described pandalid species. The description of the mitogenome of *P. edwardsii* could be the first step in increasing the genomic data available for this species, increasing our knowledge of its

biology and help elucidate the taxonomy of the genus and the family.

MATERIALS AND METHODS

Sample collection and sequencing

Specimens of *P. edwardsii* were collected near the coast of Motril, southern Spain and kept in ice on the fishing boat after capture. DNA was extracted immediately after the arrival of the samples at port. For this, a sample of muscle tissue of a single individual was homogenised by grinding on liquid nitrogen and genomic DNA was extracted with the Quick-DNA™ Miniprep Plus Kit (D4069, Zymo Research, Irvine, CA, USA) using the solid tissue protocol. DNA quality was assessed by a NanoDrop 2000 (Thermo Fisher Scientific, Waltham, MA, USA) and 1% (w/v) agarose gel. High-quality DNA libraries were prepared using the Illumina TruSeq PCR-Free kit (Illumina, San Diego, CA, USA). A paired-end protocol was used to run the library on an Illumina HiSeq 2000 sequencer (Illumina), which was performed by Macrogen (Seoul, Korea).

Assembly and annotation of mitochondrial genome

The mitogenome assembly, annotation, and analysis were performed following some of the recommendations found in Baeza (2022). *De novo* mitogenome assembly was achieved using the pipeline GetOrganelle v1.7.6.1 (Jin *et al.*, 2020), with k-mer sizes of 21, 45, 65, 85, and 105, and the entire mitogenome of *Plesionika sindoi* (accession MH714453) as a seed. The assembled genome was annotated using MITOS (http://mitos.bioinf.uni-leipzig.de/index.py) (Bernt *et al.*, 2013) and MITOS2 (http://mitos2.bioinf.uni-leipzig.de/index.py) (Donath *et al.*, 2019) selecting the invertebrate genetic code which includes the tRNA genes annotations derived from the MiTFi pipeline (Jühling *et al.*, 2012). For manual curation, the annotated start and stop codons were corrected using Geneious Prime 2022.0.2 (https://www.geneious.com/) with the translated sequence obtained from Expasy Translate Tool (https://web.expasy.org/translate/).

Analysis of mitochondrial genome

We used GenomeVx (http://wolfe.ucd.ie/GenomeVx/) (Conant & Wolfe, 2008) to construct a visual representation of the genome. Mitogenomes of the species that belong to the infraorder Caridea were retrieved from the GenBank database, as well as the mitogenome of *Stenopus scutellatus* Rankin, 1898 (infraorder Stenopodidea), which was used as an outgroup. We only used the annotated genomes in the subsequent analysis, comprising a total of 113 genomes (Supplementary material Table S1). We recovered the gene order in the different caridean species from the GenBank files using MitoPhAST v3.0 (Tan *et al.*, 2015). We used Mauve v3.0 (Darling *et al.*, 2004) to aligned the different mitogenomes, detect conserved genomic regions, and analyse their rearrangements. Nucleotide composition of the genomes and genes were obtained with Geneious. GC and AT skew were calculated according to Perna & Kocher (1995): AT skew=(A–T)/(A+T); GC skew=(G–C)/(G+C). GC and AT skew graphs were produced using the commandline

client for Genskew (Genskew_cc) (https://genskew.csb.uni-vie.ac.at/).

For PCGs, codon usage was calculated using Codon Usage (https://www.bioinformatics.org/sms2/codon_usage.html) and the codon usage bias was estimated with the relative synonymous codon usage (RSCU), which was calculated using MEGA11 (Tamura *et al.,* 2021). The Ka:Ks ratio compares the nonsynonymous (Ka) and synonymous (Ks) substitutions rates and indicates whether a region is under purifying selection (Ka:Ks < 1), diversifying selection (Ka:Ks > 1), or neutral mutation (Ka:Ks = 1). We calculated the Ka:Ks ratio using the software KaKs calculator 2.0 (Zhang *et al.,* 2006), comparing the mitogenomes of *P. edwardsii* with that of *P. sindoi*. The secondary structure of the annotated tRNAs was graphically visualised using ViennaRNA Web Services forna (http://www.viennarna.at/forna/) (Kerpedjiev *et al.,* 2015).

The analysis of the putative control region was focused on the detection of repeats sequences, the visualization of its secondary structure and the evaluation of previously described conserved sequences. We detected microsatellites using the Microsatellite repeats finder (http://insilico.ehu.es/mini_tools/micro-satellites/) and larger repeats were detected using the Tandem Repeats Finder (https://tandem.bu.edu/trf/trf.html) (Benson, 1999). We predicted the secondary structure of the CRs using Mfold (http://www.mfold.org/mfold/applications/dna-fold-ing-form.php); when there were more than one possible secondary structure the one with the lowest free energy was used for further analysis. We used Geneious to align the control regions of the different species under analysis and create dot plot graphics. RNAalifold (http://rna.tbi.univie.ac.at/cgi-bin/RNAWeb-Suite/RNAalifold.cgi) was used to visualise the number of compatible and incompatible pairs in the secondary structure of the alignment of the conserved sequence block.

Mitochondrial phylogenetic tree

The phylogenetic position of *P. edwardsii* in the family Pandalidae was assessed by constructing two phylogenetic trees using the assembled mitogenome and eight other Pandalidae mitogenomes, using two species as outgroup: *Macrobrachium lanchesteri* De Man, 1911 (Palaemonidae, accession FJ797435) and *S. scutellatus* (Stenopodidea, accession OM140691). We constructed a first phylogenetic tree using the maximum-likelihood method with the complete mitogenomes based on a Clustal Omega alignment and the GTR + I + G evolutionary model as the best DNA model proposed by MEGA11, with a bootstrap of 1,000 pseudoreplicates. These results were compared with the phylogenetic tree resulting of concatenating the 13 PCGs and aligning them with MitoPhAST v3.0. Briefly, MitoPhAST extracted the 13 PCGs of the GenBank files provided and the amino acid sequences were aligned using TranslatorX (Abascal *et al.,* 2010), ambiguously-aligned regions were trimmed with Gblocks (Castresana, 2000), and the clean alignments were concatenated with FASconCAT-G (Kück & Longo, 2014). The concatenated PCG amino acid alignments were used to construct a maximum-likelihood phylogenetic tree using IQ-TREE (Nguyen *et al.,* 2015). We calculated 1,000 bootstrap pseudoreplicates to evaluate the robustness of the tree topology.

RESULTS AND DISCUSSION

The Illumina sequencing resulted in 19 million pairs of reads, comprising a total of 5.8 Gigabases of DNA. This data is available in the Sequence Read Archive (SRA) repository from NCBI (BioProject PRJNA894443, BioSample SAMN31455524, run accession number SRR22046692).

General features: structure, organization and composition

The complete mitogenome of *P. edwardsii* was 15,956 bp in length and our assembly had an average coverage of 148.7x (GenBank accession number OP087601). The mitogenome size of this species was similar to that of *P. sindoi* (15,908 bp) and in the range of other Pandalidae mitogenomes sequences deposited in the GenBank database (*Bitias brevis* (Rathbun, 1906) 15,891; *Pandalus prensor* (Stimpson, 1860) 17,194 bp). Similarly to other crustacean mitogenomes, the *P. edwardsii* mitogenome had an A+T bias, with a percentage of A = 33.4%, T = 31.8%, C = 21.1% and G = 13.6%. It included 13 PCGs, 2 rRNA genes (*rrnS* and *rrnL*), and 22 tRNA genes. The positive strand encoded most of the genes; the negative strand encoded four PCGs (*nad5, nad4, nad4l,* and *nad1*) and eight tRNA genes (*trnF, trnH, trnP, trnL1, trnV, trnQ, trnC,* and *trnY*), as well as both of the rRNA genes (Fig. 1). Gene overlaps were recorded in seven genes, overlapping between 1 and 40 bp, whereas intergenic spaces were present in 18 gene junctions ranging between 1 and 30 bp, apart from the region that was assumed to be the control region (CR) (Table 1).

Gene order

The gene order observed in *P. edwardsii* is shown in Figure 1 and Table 1. The pattern is identical to the ancestral crustacean pattern (Hickerson & Cunningham, 2000), which is shared by most of the species of Caridea, including entire families that maintain the ancestral pattern (i.e. Alvinocarididae and Atyidae). Most of the changes in the mitochondrial architecture that we have found in Caridea affect to the number and position of tRNA genes, which correlates with previous observations in different phyla (Gissi *et al.,* 2008). Some of these changes in tRNA genes position are conserved in multiple species of the same genus. We nevertheless detected that there are two species, *Thor amboinensis* (De Man, 1888) and *Hymenocera picta* (Dana, 1852), with PCGs rearrangements in comparison with the ancestral pattern shared by *P. edwardsii*. Both species present rearrangements that comprise the same PCGs (*nad6* and *cob*), as well as the neighbouring tRNA genes, *trnT* and *trnS*, and they have translocated to locations with other adjoining tRNA genes (Fig. 2). The *trnP* gene seemed to have translocated as part of this block in *H. picta* but it had translocated separately in *T. amboinensis*. The translocation found in *T. amboinensis* had been described (Zhu *et al.,* 2021), but the translocation of this same genomic region in another species makes us presume that this is the region being translocated and not the surrounding sequences. These rearrangements are consistent with the tandem-duplication/random loss model, and agree with the findings of Han *et al.* (2022) that breakpoints for recombination have a tendency to occur between tRNA genes, which show a high gene translocation rates (Tyagi *et al.,* 2020). It is possible that these translocations have only occurred in one individual and not in the entire
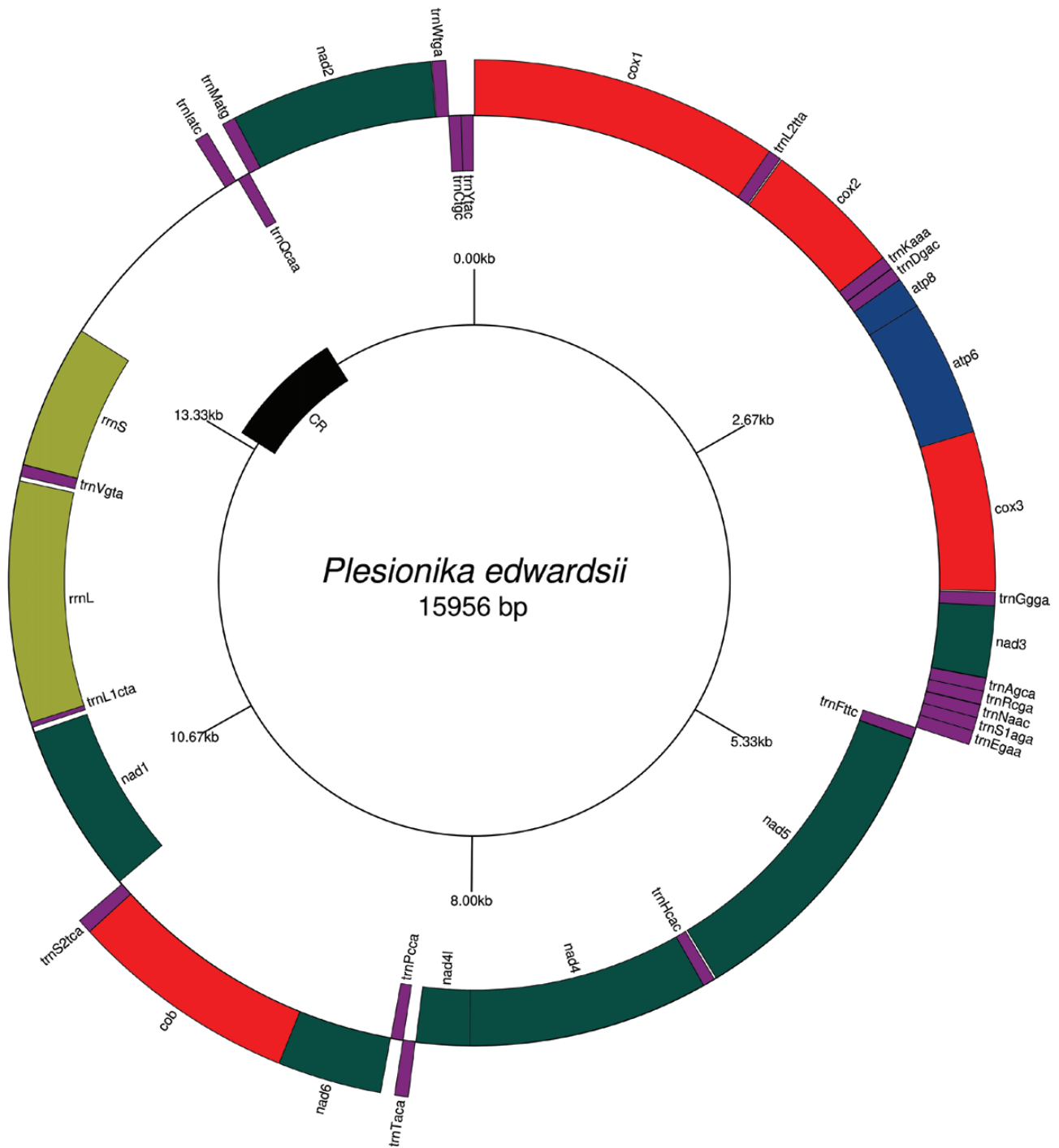
Figure 1. Visual representation of the circular mitochondrial genome of *Plesionika edwardsii* depicting its 13 protein-coding and 22 transfer-RNA genes (*trnX*) with their anticodons, 2 ribosomal RNA genes (*rrnS* and *rrnL*), and the putative control region (CR). The outer circle genes are encoded by the positive strand; the inner circle genes are encoded by the negative strand.

species considering that the mitochondrial assembly, at least in *T. amboinensis*, comes from the sequencing of a single individual (Wang *et al.*, 2020) and these changes are not shared with other species of the same monophyletic group. Future studies should further analyse these possibilities.

GC and AT-skew

The mitogenome of *P. edwardsii* presented a total GC skew of −0.215431765 and an AT skew of 0.023729465, both of

which are close to the mean value of the Caridea mitogenomes (GC skew −0.2682 ± 0.0596; AT skew 0.0558 ± 0.0442) (Supplementary material Table S1). The distribution of the GC and AT skew along the genome was similar to that of other species of Pandalidae. While the GC skew decreases reaching a minimum in the CR, the AT skew presents a minimum between the *nad3* and *nad5* genes and another partial minimum between the *cob* and *nad1* genes. Although it has been described that the origin of replication of the H-strand (OH) and the origin of the

Table 1. Genomic features of the mitochondrial genome of *Plesionika edwardsii*.

Name	Type	Start	Stop	Strand	Length (bp)	Start	Stop	Anticodon	Intergenic space
cox1	Coding	1	1533	+	1533	CGA	TAA		-5
trnL2(tta)	tRNA	1529	1594	+	66			TAA	7
cox2	Coding	1602	2289	+	688	ATG	T(AA)		0
trnK(aaa)	tRNA	2290	2356	+	67			TTT	2
trnD(gac)	tRNA	2359	2425	+	67			GTC	0
atp8	Coding	2426	2584	+	159	ATC	TAA		-7
atp6	Coding	2578	3252	+	675	ATG	TAA		-1
cox3	Coding	3252	4040	+	789	ATG	TAA		6
trG(gga)	tRNA	4047	4112	+	66			TCC	0
nad3	Coding	4113	4466	+	354	ATA	TAA		2
trnA(gca)	tRNA	4469	4533	+	65			TGC	0
trnR(cga)	tRNA	4534	4599	+	66			TCG	2
trnN(aac)	tRNA	4602	4666	+	65			GTT	0
trnS1(aga)	tRNA	4667	4733	+	67			TCT	0
trnE(gaa)	tRNA	4734	4803	+	70			TTC	3
trnF(ttc)	tRNA	4807	4872	-	66			GAA	2
nad5	tRNA	4875	6590	-	1716	ATT	TAA		12
trnH(cac)	tRNA	6603	6669	-	67			GTG	0
nad4	Coding	6670	8008	-	1339	ATG	T(AA)		-7
nad4l	Coding	8002	8298	-	297	ATG	TAA		2
trnT(aca)	tRNA	8301	8368	+	68			TGT	0
trnP(cca)	tRNA	8369	8435	-	67			TGG	2
nad6	Coding	8438	8953	+	516	ATT	TAA		-1
cob	Coding	8953	10087	+	1135	ATG	T(AA)		0
trnS2(tca)	tRNA	10088	10159	+	72			TGA	20
nad1	Coding	10180	11121	-	942	ATT	TAA		30
trnL1(cta)	tRNA	11152	11218	-	67			TAG	-40
rrnL	rRNA	11179	12515	-	1337				25
trnV(gta)	tRNA	12541	12605	-	65			TAC	1
rrnS	tRNA	12607	13405	-	799				0
CR		13406	14523	+	1118				
trnI(atc)	tRNA	14524	14590	+	67			GAT	15
trnQ(caa)	tRNA	14606	14673	-	68			TTG	2
trnM(atg)	tRNA	14676	14742	+	67			CAT	0
nad2	Coding	14743	15744	+	1002	ATT	TAA		4
trnW(tga)	tRNA	15749	15817	+	69			TCA	-1
trnC(tgc)	tRNA	15817	15884	-	68			GCA	0
trnY(tac)	tRNA	15885	15949	-	65			GTA	7

L-strand (OL) are both found in the CR in the ancestral arthropod organization (Jakovlić *et al.*, 2021), our data may point to the location of the OL. Between the *nad3* and *nad5* genes there is a stem-loop secondary structure that comprises the *trnN* and *trnS1* genes and could be acting as the OL (Supplementary material Fig. S2A). It is noteworthy that the stem includes the part of the *trnS1* gene that should form a D-loop and could explain the loss of this feature to accommodate its function as an origin of replication (Supplementary material Fig. S2B). Even if the OL of this species is located in the CR, these tRNAs and the ones found between the *cob* and *nad1* genes could be acting as alternative OLs, a feature of mitochondrial tRNA genes that has been previously hypothesized (Seligmann, 2010). Shifts in skew plots are nevertheless not ideal indicators of the position and direction

of the origin of replication (Jakovlić *et al.*, 2021), so supplementary evidences would be needed to assess this possibility.

We detected some species that have an inverted AT skew value in contrast to the skew data found in *P. edwardsii* and most caridean species: *Crangon hakodatei* (Rathbun, 1902), *Palaemon elegans* Rathke, 1836 (except for the MT340088 assembly in which there are multiple gaps), *Palaemon serenus* (Heller, 1862), *Palaemon varians* (Leach, 1814), *Rhynchocinetes durbanensis* (Gordon, 1936), *T. amboinensis* and all the available mitogenomes of *Lysmata* (*L. vittata* (Stimpson, 1860), *L. amboinensis* (De Man, 1888), *L. debelius* (Bruce, 1983), and *L. boggessi* (Rhyne & Lin, 2006)). This change in the sign of the AT skew had previously been described in *T. amboinensis, L. vittata, L. amboinensis, L. debelius,* and *L. boggessi* (Zhu *et al.*, 2021). One of the biggest
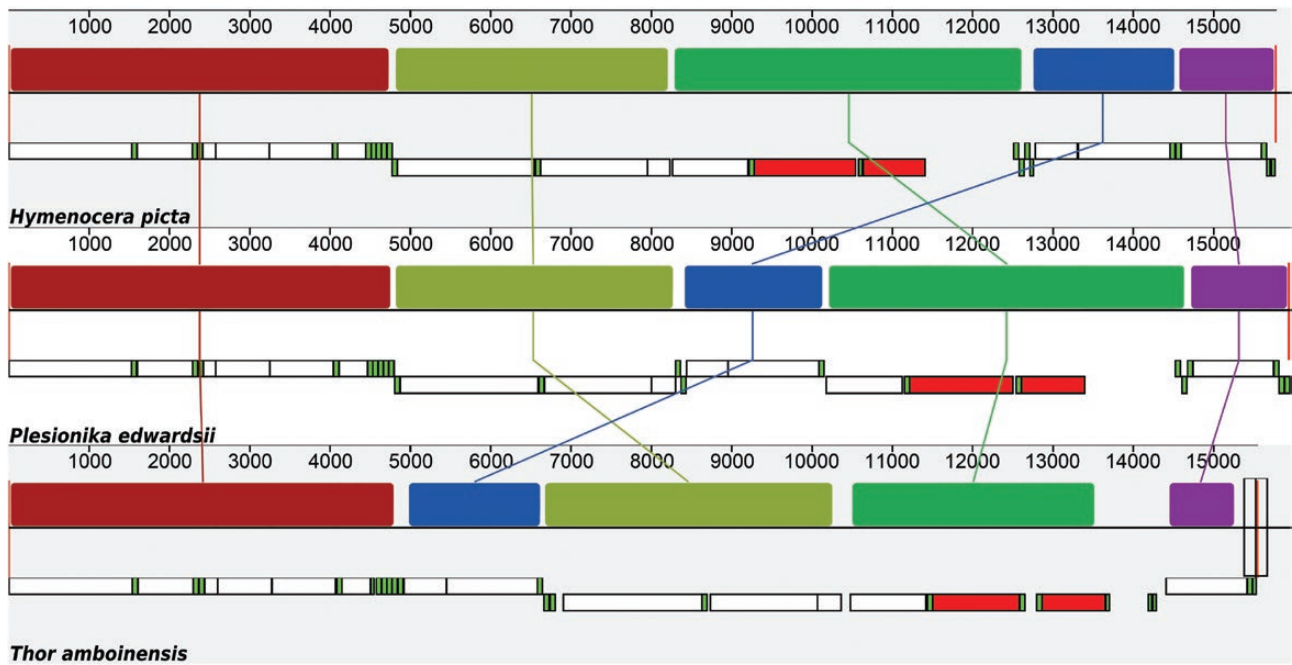
Figure 2. Mauve alignment of syntenic blocks (coloured) of the mitochondrial genomes of *Hymenocera picta*, *Plesionika edwardsii,* and *Thor amboinensis*. Whereas *P. edwardsii* maintains the ancestral gene organization, *H. picta* and *T. amboinensis* genomes show a translocation of the same genomic region.

differences in the AT skew distribution between these mitogenomes and the rest of Caridea is that, except for *T. amboinensis*, they all have a maximum of the AT skew between *nad4l* and *nad6* and the AT skew is lower than in other species between *nad6* and *cox1*. The changes in sign of the GC and AT skew values can be related to changes in the replication order of the mitochondrial DNA strands, as these changes produce an inversion in the mutational pressure of each strand (Jakovlić *et al.,* 2021). We would expect, however, that such a change would produce modifications in other parameters, such as an alternated codon usage bias which does not seem to be reflected in the published data (Zhu *et al.,* 2021).

The different AT skew found in *T. amboinensis* could be caused by a change in the mutational pressure of the translocated genes or the shifting in the position or the strand of the origins of replication (Jakovlić *et al.,* 2021). Our data suggested a change in the position of the OL, as the region of minimal AT skew in this species is located downstream to the translocated block and includes a hairpin structure (Supplementary material Fig. S2). This hairpin structure differed from those found in other carideans in that it did not include part of the *trnS1* gene, which actually presented a D-arm in *T. amboinensis*. We would expect a change in the mutational pressure of the genes in the case of a shifting in the OL. When comparing the GC and AT skew of each gene between *P. edwardsii* and *T. amboinensis*, we found that there is a change of sign in the GC skew of the *cox1* gene in *T. amboinensis*. This last species also showed a change in the magnitude of the GC skew of the genes *cob, cox2, cox3, nad2* and *nad3*, having all increased their GC skew in comparison with *P. edwardsii*. The changes in the skewness of these genes might not be correlated with a change in the OL. Shen *et al.* (2012), for example, described an AT skew shift in *cox2* without an apparent change in the origin of replication in *Alpheus japonicus* (Miers,

1879). Further analysis should determine if there has been a change in the OL and how it may be affecting distal genes, such as *cox1*, more than *nad6*, which is one of the translocated genes and its GC skew seems to remain unchanged.

Protein-coding genes

All PCGs of the *P. edwardsii* mitogenome started with an ATN start codon, with the exception of *cox1*. It is possible that this gene starts with the alternative start codon CGA that MITOS annotates in this species and that has been previously reported in other crustaceans (Baeza, 2018), including another pandalids (Sun *et al.,* 2020) and several lepidopterans. The use of alternative codons nevertheless hinders the proper characterization of this gene using only bioinformatics tools. Ten of the PCGs ended with a TAA codon, whereas three of them (*cob, cox2* and *nad4*) ended with a truncated stop codon T-- that can be poly-adenylated to form a functional TAA codon, as demonstrated in another crustacean, a species of *Armallidillum*, a terrestrial isopod (Doublet *et al.,* 2015) as well as having been widely described in metazoans. None of the PCGs found in this genome used the TAG stop codon.

The most frequently used codons in PCGs were TTA (Leu, 252 times used, 6.78% of total), TTT (Phe, $N = 202$, 5.43%), and ATT (Ile, $N = 193$, 5.19%), followed by ATA (Met), CTT (Leu), and GCT (Ala), all of them separately comprising ~3% of the total. According to codon usage, leucine was the most frequent amino acid in the mitochondrial proteins of *P. edwardsii,* accounting for 16.25% of all amino acids, followed by serine and phenylalanine. The least frequently used codons that encode amino acids were CGC (Arg, $N = 4$, 0.06%), CCG (Pro, $N = 8$, 0.05%), TGC (Cys, $N = 11$, 0.28%), and CGG (Arg, $N = 11$, 0.17%). The least frequent amino acids

being cysteine and arginine. In general, the codons NNU and NNA had a RSCU value higher than 1 (Table 2), pointing to a bias for A+T nucleotides in the third position of codons, a phenomenon already described in other species of pandalids (Sun *et al.*, 2020). The mitogenome of *P. edwardsii* had a ratio of G+C/A+T-rich codons of 0.64, lower than previously analysed mitogenomes of pandalids that ranged between 0.67 and 0.69 (Sun *et al.*, 2020), but still reflecting the preference for A+T-rich codons, which correlates with the high AT content of these genomes.

All mitochondrial PCGs Ka:Ks ratios ranged between 0.00581321 and 0.0421711, as shown in Figure 3, with *nad2* and *nad6* showing the highest ratios (0.0421711 and 0.0368343, respectively) and *atp6*, *cob*, *cox1*, and *nad1* showing the lowest ratios (all between 0.00581321 and 0.00630791). These ratios indicated that all PCGs were under purifying selection with the greatest ratios indicating less mutation constraints on these genes. *Nad6* is one of the three fast-evolving mitochondrial genes (*atp8*, *nad4l*, and *nad6*) (Jakovlić *et al.*, 2021), and there-

fore its ratio correlates with a weaker purifying selection. The highest ratios in our results were still lower than previous results of the comparison of two species of *Pandalus* (Cronin *et al.*, 2022), which correlates with our observations that the mitogenomes of this last genus seem to have undergone more changes than *Plesionika*, with a greater variability of its genomic features. In general, the NADH dehydrogenase subunits seem to be under weaker purifying selection in this family as both our results and those of the genus *Pandalus* (Cronin *et al.*, 2022), point to these genes having higher Ka:Ks ratios.

Transfer RNA and ribosomal RNA genes

MITOS annotated the complete set of 22 tRNA genes found in most metazoans in the mitogenome of *P. edwardsii*. The total length of the tRNAs was 1,475 bp, which correlates with other caridean shrimps. These tRNA genes ranged from 65 bp (*trnN* and *trnY*) to 72 bp (*trnS2*) in length. All the genes could be fold into a standard tRNA secondary structure with the exception of

Table 2. Codon usage and relative synonymous codon usage summary of the protein-coding genes in the mitochondrial genome of *Plesionika edwardsii*.

AA	Codon	N	/1000	Fraction	RSCU	AA	Codon	N	/1000	Fraction	RSCU
Ala	GCG	26	6.99	0.10	0.4111	Pro	CCG	8	2.15	0.05	0.2177
	GCA	55	14.79	0.22	0.8696		CCA	29	7.8	0.2	0.7891
	GCT	115	30.93	0.45	1.8182		CCT	82	22.05	0.56	2.2313
	GCC	57	15.33	0.23	0.9012		CCC	28	7.53	0.19	0.7619
Cys	TGT	29	7.8	0.72	1.4500	Gln	CAG	14	3.77	0.19	0.3889
	TGC	11	2.96	0.28	0.5500		CAA	58	15.6	0.81	1.6111
Asp	GAT	54	14.52	0.74	1.4795	Arg	CGG	11	2.96	0.17	0.6984
	GAC	19	5.11	0.26	0.5205		CGA	31	8.34	0.49	1.9683
Glu	GAG	28	7.53	0.38	0.7568		CGT	17	4.57	0.27	1.0794
	GAA	46	12.37	0.62	1.2432		CGC	4	1.08	0.06	0.2540
Phe	TTT	202	54.33	0.66	1.3160	Ser	AGG	39	10.49	0.11	0.8619
	TTC	105	28.24	0.34	0.6840		AGA	52	13.99	0.14	1.1492
Gly	GGG	71	19.1	0.28	1.1270		AGT	34	9.14	0.09	0.7514
	GGA	83	22.32	0.33	1.3175		AGC	14	3.77	0.04	0.3094
	GGT	67	18.02	0.27	1.0635		TCG	24	6.46	0.07	0.5304
	GGC	31	8.34	0.12	0.4921		TCA	66	17.75	0.18	1.4586
His	CAT	40	10.76	0.49	0.9877		TCT	106	28.51	0.29	2.3425
	CAC	41	11.03	0.51	1.0123		TCC	27	7.26	0.07	0.5967
Ile	ATT	193	51.91	0.72	1.4349	Thr	ACG	21	5.65	0.1	0.4038
	ATC	76	20.44	0.28	0.5651		ACA	72	19.37	0.35	1.3846
Lys	AAG	23	6.19	0.28	0.5542		ACT	85	22.86	0.41	1.6346
	AAA	60	16.14	0.72	1.4458		ACC	30	8.07	0.14	0.5769
Leu	TTG	63	16.94	0.10	0.6258	Val	GTG	42	11.3	0.16	0.6364
	TTA	252	67.78	0.42	2.5033		GTA	91	24.48	0.34	1.3788
	CTG	32	8.61	0.05	0.3179		GTT	103	27.7	0.39	1.5606
	CTA	78	20.98	0.13	0.7748		GTC	28	7.53	0.11	0.4242
	CTT	132	35.5	0.22	1.3113	Trp	TGG	22	5.92	0.22	0.4490
	CTC	47	12.64	0.08	0.4669		TGA	76	20.44	0.78	1.5510
Met	ATG	56	15.06	0.29	0.5743	Tyr	TAT	83	22.32	0.63	1.2672
	ATA	139	37.39	0.71	1.4256		TAC	48	12.91	0.37	0.7328
Asn	AAT	83	22.32	0.63	1.2576	Stop	TAG	0	0	0.00	0.0000
	AAC	49	13.18	0.37	0.7424		TAA	10	2.69	1.00	2.0000
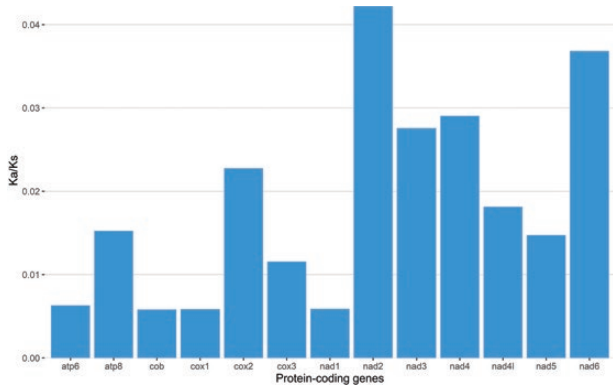
Figure 3. Analysis of the selective pressure of the different protein-coding genes of the mitochondrial genome of *Plesionika edwardsii*, values of Ka (number of nonsynonymous substitutions per nonsynonymous site)/Ks (number of synonymous substitutions per synonymous site) of each protein-coding gene, calculated comparing the mitochondrial genomes of *P. edwardsii* and *Plesionika sindoi*.

trnS1, which is missing the DHU-arm (Supplementary material Fig. S3), a common feature in metazoan mitogenomes that has been described in other species of Pandalidae (Sun *et al.*, 2020; Cronin *et al.*, 2022). These tRNAs carried the same anticodons as previously described in *Pandalus platyceros* Brandt, 1851 (Cronin *et al.*, 2022).

The *rrnS* and *rrnL* genes identified had similar lengths to those of other previously described carideans sequences, with 799 bp and 1337 bp, respectively. They both had higher A+T content than G+C, with the *rrnS* gene having A+T = 63.6% and G+C = 36.4% and the *rrnL* gene having A+T = 70.8% and G+C = 29.2%.

Non-coding region

The 1,118 bp-long region without any gene annotations found between the *rrnS* gene and the *trnI* gene was assumed to be the control region (CR) as its location corresponds with the location of the CR in other carideans. Its length was within the range of the CR of other available Pandalidae mitogenomes (*Pandalus prensor* 599 bp, *Parapandalus sp. SS-2019* 1,229 bp), although somewhat larger than the one found in *Plesionika sindoi* (1,069 bp). It is an A+T rich region, with a base composition of A = 40.6%, T = 34.9%, C = 14.3%, and G = 10.2%. According to the microsatellite analysis of this region there are 12 simple sequence repeats with similar sequences to those found in *Macrobrachium nipponense* De Haan, 1849 (Ma *et al.*, 2011), *P. platyceros* (Cronin *et al.*, 2022), and *Synalpheus microneptunus* Hultgren, Macdonald & Duffy, 2011 (Chak *et al.*, 2020), mostly repetitions of AT and A (Supplementary material Fig. S4).

According to (Sun *et al.*, 2020), the control region of four pandalids (*B. brevis*, *Chlorotocus crassicornis* (Costa, 1871), *Heterocarpus ensifer* (Milne-Edwards, 1881), and *Pandalus borealis* (Krøyer, 1838)) presented a conserved sequence block (CSB) that could be implicated in the replication of these species. The presence of a CSB in a noncoding region has been used as location marker of the origin of replication in another metazoan lineage (Ghiselli *et al.*, 2013). We therefore analysed the presence of this block in *P. edwardsii* by constructing an alignment with other Panadalidae species (*B. brevis*, *C. crassicornis*, *H. ensifer*, *P. borealis*, *P. prensor*, *Pandalus japonicuss* (Balss, 1914), *Parapandalus sp.*

SS-2019, and *P. sindoi*), excluding *Pandalus hypsinotus* (Brandt, 1851) as no similar sequence was found in this species. In our analysis, the consensus sequence of the CRs included a 104 bp sequence with a 94.2% similarity to the previously described CSB. While this block remains the most conserved part of the CR, in our analysis the similarity is 35.8%, lower than previously described (69.23%), but still has a much higher similarity than the complete CR (12.7%). The sequence found in *P. edwardsii* was one of the most distant to those of other species, only surpassed by the one found in *P. japonicus*. We found that in the secondary structure of this block there is a stem-loop structure that is maintained in different Pandalidae species, even in the two species with the lower similarity. The relative location of this structure also seems to be conserved. These species have other stem-loop structures in this region but their localization is more variable. It is noteworthy that in the case of *P. edwardsii*, although the sequence is less similar, the SNPs in relation to the consensus of one side of the stem are compensated with contrary SNPs in the other side of the stem, showing a possible evolution pressure to maintain this structure. We tested this possibility with the software RNAalifold, which points to the presence of compatible and incompatible pairs in the secondary structure of an alignment. We found that most of the nucleotides that form the stem are also the most conserved ones with some instances of compensatory mutations (Fig. 4).

The CR seemed to have changed by the larger presence of microsatellite repeats in *P. hypsinotus*, where it contained a larger loop formed by 66 repeats of the dinucleotide TA. The location of this loop, however, did not correlate with the one formed by the CSB, although this could be due to the presence of a 60 bp region comprised of TG repeats and a 160 bp region comprised of TGTA repeats that may have switched its location. We did not find other pandalid species in which the microsatellite repeats found in the CR form a stem-loop structure, although the loop formed by the CSB has some regions of poly-A and poly-T (≤ 5 bp).

For comparison, we tested the CR of species of Alvinocarididae with mitogenomes available. Sun *et al.* (2018) compared seven species of Alvinocarididae and detected two CSBs in the CR, both of which showed more similarity that the CSB we analysed in Pandalidae (CSB1 87.0% sequence identity and CSB2 74% sequence identity). Both of these CSBs are also larger than the 104 bp CSB described in Pandalidae. In our analysis we included six assemblies of five species, making a total of 13 mitogenomes of this family: *Alvinocaris chelys* (Komai & Chan, 2010), *A. kexueae* (Wang & Sha, 2017), *A. longirostris* (Kikuchi & Ohta, 1995), *Chorocaris paulexa* (Martin & Shank, 2005), *Manuscaris liui* (Wang & Sha, 2016), *Mirocaris indica* (Komai *et al.*, 2006), *Nautilocaris saintlaurentae* (Komai & Segonzac, 2004), *Opaepele loihi* (Williams & Dobbs, 1995), *Rimicaris exoculata* (Williams & Rona, 1986), *R. kairei* (Watabe & Hashimoto, 2002), *R. variabilis* (Komai & Tsuchida, 2015) (MH714460, MN419306), and *Shinkaicaris leurokolos* (Kikuchi & Hashimoto, 2000). The CSB1 showed a 56.2% sequence identity and the CSB2 a 47.9% sequence identity, less identity percentage than previously described. We investigated if these two CSBs could also form hairpin structures, both did and they showed high conservation of the stem and some instances of compensatory mutations. We could find these secondary structures in the CR
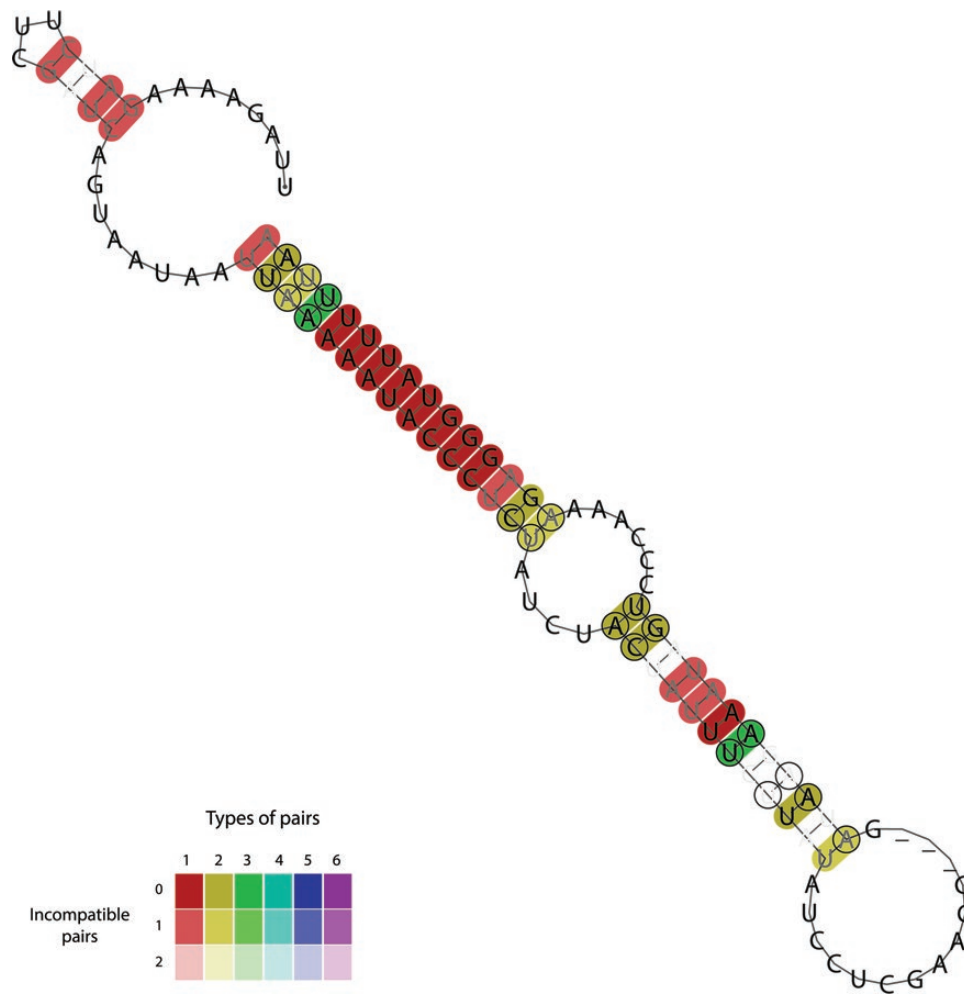
Figure 4. Secondary structure of the consensus sequence of the alignment of the conserved block region found in the control region of *Bitias brevis*, *Chlorotocus crassicornis*, *Heterocarpus ensifer*, *Plesionika edwardsii*, *Plesionika sindoi*, *Pandalus japonicus*, *Pandalus prensor*, and *Parapandalus sp. SS-2019*, predicted by RNAalifold and showing the number of types of pairs and incompatibilities found in the alignment.

of all the species analysed. These hairpins were formed mainly by poly-A and poly-T. The relative location of these hairpins was nevertheless different to the one found in Pandalidae. The hairpin in Alvinocarididae shows a more central location inside the CR, whereas the one found in Pandalidae was located near the 3′ end of the region.

We wanted to investigate if a similar feature of a CSB that formed a stem-loop structure was also present in the caridean species that have more than one CR. Moreover, if the canonical CR common to most caridean species and the additional CRs shared any conserved sequence that could point to the origin of the additional CRs. In *L. vittata*, for example, three CRs had been described, one found between *rrnS* and *trnI* (CR1), that corresponded with the one found in the rest of Caridea and two regions found between *cox1* and *cox2* and divided by the *trnL* gene (CR2 and CR3 respectively) (Chen *et al.*, 2021; Zhu *et al.*, 2021). When comparing the CR2 and CR3 regions between the assembly from a specimen from the Fujian province, China (MT478132) (Zhu *et al.*, 2021) and the assembly from a specimen from the Guandong province (MW285083) (Chen *et al.*, 2021), however, we found that the CR2 and CR3 could be aligned as a continuous sequence

(Supplementary material Fig. S5A). We therefore took into account CR2 and CR3, as well as the *trnL2* that was separating them, as a single region (CR2+CR3 region). When comparing the two assemblies we found that the similarity of the CR1 was 99.7%, whereas the similarity of the CR2 and CR3 was 84.3%. In the Fujian assembly 25.8% of the CR2+CR3 region was formed by tandem repeats, with the longest period size being 227 bp. In the Guandong assembly there were less tandem repeats in this region, accounting for 20.1% of the CR2+CR3 region and 113 bp being the longest period size. This was due to indels in this region that affected mainly the tandem repeats (Supplementary material Fig. S5B). These repeats could have actually hindered the assembly of this region causing the difference in length between the two assemblies. The alignment between the CR1 and the CR2+CR3 resulted in a 55.5% similarity in the Guandong assembly and a 56.7% similarity in the Fujian assembly, there did not seem to be any particular region with high similarity and in fact most of the similarities seemed to come down to poly-A, poly-T and AT repeats. The CR1 of *L. vittata* had a stem-loop structure towards the 3′ end of the region, in accordance with what we have described in other species of this infraorder. The CR2+CR3 region, on the
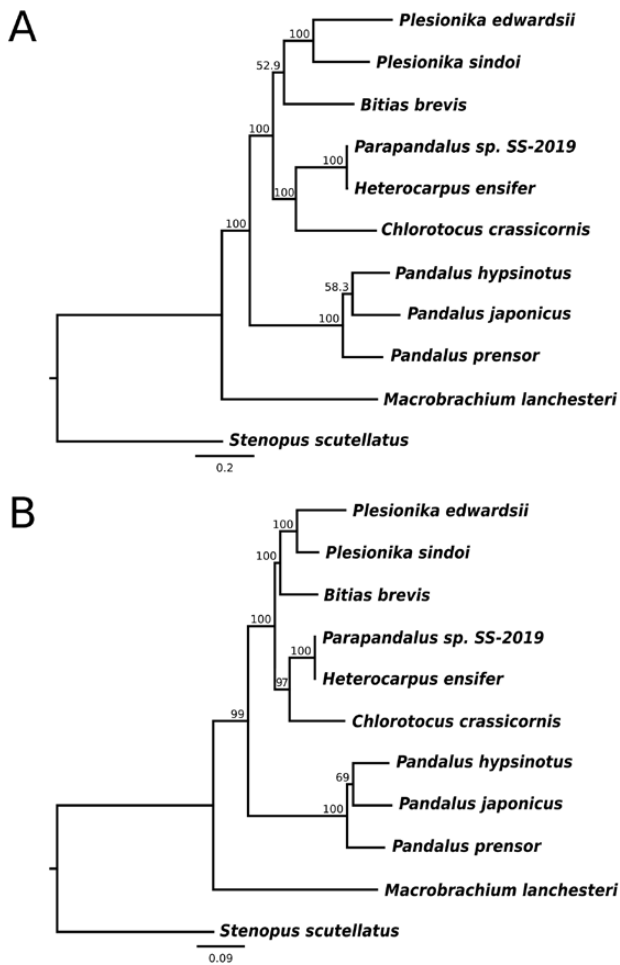
Figure 5. Phylogenetic trees of the mitochondrial genomes of the pandalid species with annotated sequences in the GenBank database using *Macrobrachium lanchesteri* (family Palaemonidae) and *Stenopus scutellatus* (infraorder Stenopodidea), both with 1,000 bootstrap pseudoreplicates, as outgroups. Phylogenetic tree derived from a maximum-likelihood analysis over an alignment of the complete mitochondrial genomes (**A**). Phylogenetic tree derived from a maximum-likelihood analysis of the amino acid alignment of 13 concatenated protein-coding genes (**B**).

other hand, had both a stem-loop structure near the 5′ end and another one near the 3′ end.

None of the tandem repeats found in *L. vittata* were found in any of the CR2 of other *Lysmata* species. The similarity between CR1 and CR2 was low in all of the other *Lysmata* species. The CR2 alignment between species was not able to detect conserved regions. In the case of CR1 alignment, excluding *L. vittata*, which was the most distant, there was a conserved region that could form a stem-loop structure, just as we have described in other families.

Phylogenetic analysis

Cronin *et al.* (2022) described the phylogenetic relationships of the mitogenomes from the species of Caridea available in the Genbank database. As a result, we focused on the phylogenetic position of the newly assembled mitogenome of *P. edwardsii* in relation to the available mitogenomes of other species of Pandalidae. We constructed two different phylogenetic trees, one with the entire mitogenomes of the selected species and another one with the concatenated PCGs (Fig. 5). The topology of both trees was identical, with *P. edwardsii* and *P. sindoi* forming a monophyletic group that groups with *B. brevis*, *C. crassicornis*, *H. ensifer*, and *Parapandalus sp. SS-2019*, with *Pandalus* being more distant to the rest of the species of Pandalidae.

Our analyses show that the mitogenome of *P. edwardsii* shares similar features with other species of Caridea. This new resource, paired with an increase in the available genomic data of *Plesionika*, could nonetheless help clarify the taxonomy of this genus, as well as, improve our understanding of the biology of *P. edwardsii*, important for its conservation and the management of its fisheries. Our study also highlights the need to further investigate the already available data of crustacean mitogenomes to increase our understanding of their genetic characteristics.

SUPPLEMENTARY MATERIAL

Supplementary material is available at *Journal of Crustacean Biology* online.

S1 Table. GC and AT skew value of the selected caridean mitogenomes.

S2 Figure. Analysis of the regions with minimal AT skew in the mitogenomes of *Plesionika edwardsii* and *Thor amboinensis*.

S3 Figure. Secondary structure of the tRNA genes of the mitogenome of *Plesionika edwardsii*.

S4 Figure. Secondary structure and highlighted sequences of the control region of *Plesionika edwardsii*.

S5 Figure. Analysis of the control region of two assemblies of *Lysmata vittata*.

ACKNOWLEDGEMENTS

REFERENCES

Abascal, F., Zardoya, R. & Telford, M.J. 2010. TranslatorX: Multiple alignment of nucleotide sequences guided by amino acid translations. *Nucleic Acids Research*, **38**: 7–13.

Abelló, P., Valladares, F.J. & Castellón, A. 1988. Analysis of the structure of decapod crustacean assemblages off the Catalan coast (North-West Mediterranean). *Marine Biology*, **98**: 39–49.

Ahamed, F., Cardoso, I.A., Ahmed, Z.F., Hossain, M.Y. & Ohtomi, J. 2017. An overview of the genus *Plesionika* Bate, 1888 (Decapoda, Caridea, Pandalidae) in Asian waters. *Zootaxa*, **4221**: 575–593.

Baeza, J.A. 2018. The complete mitochondrial genome of the Caribbean spiny lobster. *Panulirus argus*. *Scientific Reports*, **8**: 17690 [https://doi.org/10.1038/s41598-018-36132-6].

Baeza, J.A. 2022. An introduction to the Special Section on Crustacean Mitochondrial Genomics: Improving the assembly, annotation, and characterization of mitochondrial genomes using user-friendly and open-access bioinformatics tools, with decapod crustaceans as an

example. *Journal of Crustacean Biology*, **42**: [https://doi.org/10.1093/jcbiol/ruac012].

Benson, G. 1999. Tandem repeats finder: a program to analyze DNA sequences. *Nucleic Acids Research*, **27**: 573–580.

Bernt, M., Donath, A., Jühling, F., Externbrink, F., Florentz, C., Fritzsch, G., Pütz J., Middendorf, M., Stadler, P.F. 2013. MITOS: Improved *de novo* metazoan mitochondrial genome annotation. *Molecular Phylogenetics and Evolution*, **69**: 313–319.

Boore, J.L. 1999. Animal mitochondrial genomes. *Nucleic Acids Research*, **27**: 1767–1780.

Brandt, J.F. 1851. Krebse. In: Middendorff, A.T. von, *Reise in den äussersten Norden und Osten Sibiriens während der Jahre 1843 und 1844 mit allerhöchster Genehmigung auf Veranstaltung der Kaiserlichen Akademie der Wissenschaften zu St. Petersburg ausgeführt und in Verbinding mit vielen Gelehrten herausgegeben*, **Vol. 2**(1): 77–148, pls. 5, 6. St. Petersburg.

Castresana, J. 2000. Selection of conserved blocks from multiple alignments for their use in phylogenetic analysis. *Molecular Biology and Evolution*, **17**: 540–552.

Chak, S.T.C., Barden, P. & Baeza, J.A. 2020. The complete mitochondrial genome of the eusocial sponge-dwelling snapping shrimp *Synalpheus microneptunus*. *Scientific Reports*, **10**: 7744 [https://doi.org/10.1038/s41598-020-64269-w].

Chakraborty, R.D. & Kuberan, G. 2021. Notes on *Plesionika alcocki* (Anderson, 1896) and *Plesionika narval* (Fabricius, 1787) from the southern coast of India. *International Journal of Fisheries and Aquatic Studies*, **9**: 281–287.

Chakraborty, R.D., Chan, T.Y., Maheswarudu, G., Kuberan, G., Purushothaman, P., Chang, S.C. & Jomon, S. 2015. On *Plesionika quasigrandis* Chace, 1985 (Decapoda, Caridea, Pandalidae) from southwestern India. *Crustaceana*, **88**: 923–930.

Chan, T.Y. & Yu, H.P. 1991. Two similar species: *Plesionika edwardsii* (Brandt, 1851) and *Plesionika crosnieri*, new species (Crustacea: Decapoda: Pandalidae). *Proceedings of the Biological Society of Washington*, **104**: 545–555.

Chen, J., Xian, C., Luo, Y. & Lin, M. 2021. Characterization of the complete mitochondrial genome of *Lysmata vittata* (Decapoda: Hippolytidae). *Mitochondrial DNA Part B*, **6**: 1718–1720.

Colloca, F. 2002. Life cycle of the deep-water pandalid shrimp *Plesionika edwardsii* (Decapoda, Caridea) in the central Mediterranean Sea. *Journal of Crustacean Biology*, **22**: 775–783.

Conant, G.C. & Wolfe, K.H. 2008. GenomeVx: simple web-based creation of editable circular chromosome maps. *Bioinformatics*, **24**: 861–862.

Cronin, T.J., Jones, S.J.M. & Baeza, J.A. 2022. The complete mitochondrial genome of the spot prawn, *Pandalus platyceros* Brandt in von Middendorf, 1851 (Decapoda: Caridea: Pandalidae), assembled from linked-reads sequencing. *Journal of Crustacean Biology*, **42**: [https://doi.org/10.1093/jcbiol/ruac003].

Curole, J.P. & Kocher, T.D. 1999. Mitogenomics: Digging deeper with complete mitochondrial genomes. *Trends in Ecology and Evolution*, **14**: 394–398.

Darling, A.C.E., Mau, B., Blattner, F.R. & Perna, N.T. 2004. Mauve: Multiple alignment of conserved genomic sequence with rearrangements. *Genome Research*, **14**: 1394–1403.

De Grave, S. & Fransen C.H.J.M. 2011. Carideorum Catalogus: the recent species of the dendrobranchiate, stenopodidean, procarididean and caridean shrimps (Crustacea: Decapoda). *Zoologische Mededelingen*, **85**: 195–589.

Donath, A., Jühling, F., Al-Arab, M., Bernhart, S.H., Reinhardt, F., Stadler, P.F., Middendorf M., Bernt, M. 2019. Improved annotation of protein-coding genes boundaries in metazoan mitochondrial genomes. *Nucleic Acids Research*, **47**: 10543–10552.

Doublet, V., Ubrig, E., Alioua, A., Bouchon, D., Marcadé, I. & Maréchal-Drouard, L. 2015. Large gene overlaps and tRNA processing in the compact mitochondrial genome of the crustacean *Armadillidium vulgare*. *RNA Biology*, **12**: 1159–1168.

Elson, J.L. & Lightowlers, R.N. 2006. Mitochondrial DNA clonality in the dock: can surveillance swing the case? *Trends in Genetics*, **22**: 603–607.

Fanelli, E. & Cartes, J. 2004. Feeding habits of pandalid shrimps in the Alboran Sea (SW Mediterranean): influence of biological and environmental factors. *Marine Ecology Progress Series*, **280**: 227–238.

García-Rodríguez, M., Esteban, A. & Perez Gil, J.L. 2000. Considerations on the biology of *Plesionika edwardsii* (Brandt, 1851) (Decapoda, Caridea, Pandalidae) from experimental trap catches in the Spanish western Mediterranean Sea. *Scientia Marina*, **64**: 369–379.

Ghiselli, F., Milani, L., Guerra, D., Chang, P.L., Breton, S., Nuzhdin, S.V. & Passamonti, M. 2013. Structure, transcription, and variability of metazoan mitochondrial genome: perspectives from an unusual mitochondrial inheritance system. *Genome Biology and Evolution*, **5**: 1535–1554.

Gissi, C., Iannelli, F. & Pesole, G. 2008. Evolution of the mitochondrial genome of Metazoa as exemplified by comparison of congeneric species. *Heredity*, **101**: 301–320.

González, J.A., Carrillo, J., Santana, J.I., Martínez-Baños, P. & Vizuete, F. 1992. La pesquería de Quisquilla, *Plesionika edwardsii* (Brandt, 1851), con tren de nasas en el Levante español. Ensayos a pequeña escala en Canarias. *Scientia Marina*, **170**: 3–31.

González, J.A., Pajuelo, J.G., Triay-Portella, R., Ruiz-Díaz, R., Delgado, J., Góis, A.R. & Martins, A. 2016. Latitudinal patterns in the life-history traits of three isolated Atlantic populations of the deep-water shrimp *Plesionika edwardsii* (Decapoda, Pandalidae). *Deep-Sea Research Part I: Oceanographic Research Papers*, **117**: 28–38.

Han, L., Yang, Y., Li, H., Zhou, X., Zhou, M., Liu, T., Lu, Y., Wang, Q., Yang, S., Shi, M., Li, X., Du, S., Guan, C., Zhang, Y., Guo, W., Wang, J., Chai, H., Lan, T., Liu, H., Liu, Q., Sun, H. & Hou, Z. 2022. Gene rearrangements in the mitochondrial genome of ten ascaris species and phylogenetic implications for Ascaridoidea and Heterakoidea families. *International Journal of Biological Macromolecules*, **221**: 1394–1403

Hickerson, M.J. & Cunningham, C.W. 2000. Dramatic mitochondrial gene rearrangements in the Hermit crab *Pagurus longicarpus* (Crustacea, Anomura). *Molecular Biology and Evolution*, **17**: 639–644.

Holthuis, L.B. 1980. FAO species catalogue. Vol. 1. Shrimps and prawns of the world. An annotated catalogue of species of interest to fisheries. *FAO Fisheries Synopsis* **125**: 144–145.

Jakovlić, I., Zou, H., Zhao, X.M., Zhang, J., Wang, G.T. & Zhang, D. 2021. Evolutionary history of inversions in directional mutational pressures in crustacean mitochondrial genomes: Implications for evolutionary studies. *Molecular Phylogenetics and Evolution*, **164**: 107288. [https://doi.org/10.1016/J.YMPEV.2021.107288].

Jin, J.J., Yu, W.B., Yang, J.B., Song, Y., Depamphilis, C.W., Yi, T.S. & Li, D.Z. 2020. GetOrganelle: A fast and versatile toolkit for accurate de novo assembly of organelle genomes. *Genome Biology*, **21**: [https://doi.org/10.1186/s13059-020-02154-5].

Jühling, F., Pütz J., Bernt M., Donath A., Middendorf M., Florentz C. & Stadler P.F. 2012. Improved systematic tRNA gene annotation allows new insights into the evolution of mitochondrial tRNA structures and into the mechanisms of mitochondrial genome rearrangements. *Nucleic Acids Research*, **40**: 2833–2845

Kerpedjiev, P., Hammer, S. & Hofacker, I.L. 2015. Forna (force-directed RNA): Simple and effective online RNA secondary structure diagrams. *Bioinformatics*, **31**: 3377–3379.

Kück, P. & Longo, G.C. 2014. FASconCAT-G: Extensive functions for multiple sequence alignment preparations concerning phylogenetic studies. *Frontiers in Zoology*, **11**: [https://doi.org/10.1186/s12983-014-0081-x].

Liao, Y., De Grave, S., Ho, T.W., Ip, B.H.Y., Tsang, L.M., Chan, T.Y. & Chu, K.H. 2017. Molecular phylogeny of Pasiphaeidae (Crustacea, Decapoda, Caridea) reveals systematic incongruence of the current classification. *Molecular Phylogenetics and Evolution*, **115**: 171–180.

Ma, K., Feng, J., Lin, J. & Li, J. 2011. The complete mitochondrial genome of *Macrobrachium nipponense*. *Gene*, **487**: 160–165.

Martins, H.R. & Hargreaves, P.M. 1991. Shrimps of the families Pandalidae and Hippolytidae (Crustacea: Decapoda) caught in benthic traps off the Azores. *Arquipelago-Life and Earth Sciences*, **9**: 47–61.

Nguyen, L.T., Schmidt, H.A., von Haeseler, A. & Minh, B.Q. 2015. IQ-TREE: A fast and effective stochastic algorithm for estimating maximum-likelihood phylogenies. *Molecular Biology and Evolution*, **32**: 268–274.

Perna, N.T. & Kocher, T.D. 1995. Patterns of nucleotide composition at fourfold degenerate sites of animal mitochondrial genomes. *Journal of Molecular Evolution*, **41**: 353–358.

Santana, J., González, J., Lozano, I. & Tuset, V. 1997. Life history of *Plesionika edwardsii* (crustacea, decapoda, Pandalidae) around the Canary Islands, Eastern central Atlantic. *South African Journal of Marine Science*, **18**: 39–48.

Santos, R., Medeiros-Leal, W., Novoa-Pabon, A., Pinho, M., Isidro, E. & Melo, O. 2021. Unraveling distributional patterns and life-history traits of a deep-water shrimp *Plesionika edwardsii* (Decapoda, Pandalidae) under unexploited virgin conditions: a benchmark for fisheries management. *Nauplius*, **29**: [https://doi.org/10.1590/2358-2936e2021008].

Seligmann, H. 2010. Mitochondrial tRNAs as light strand replication origins: Similarity between anticodon loops and the loop of the light strand replication origin predicts initiation of DNA replication. *BioSystems*, **99**: 85–93.

Shen, X., Li, X., Sha, Z.L., Yan, B.L. & Xu, Q.H. 2012. Complete mitochondrial genome of the Japanese snapping shrimp *Alpheus japonicus* (Crustacea: Decapoda: Caridea): Gene rearrangement and phylogeny within Caridea. *Science China Life Sciences*, **55**: 591–598.

Silva, J.M. da, Santos, A. dos, Cunha, M.R., Costa, F.O., Creer, S. & Carvalho, G.R. 2013. Investigating the molecular systematic relationships amongst selected *Plesionika* (Decapoda: Pandalidae) from the Northeast Atlantic and Mediterranean Sea. *Marine Ecology*, **34**: 157–170.

Sun, S.E., Cheng, J., Sun, S. & Sha, Z. 2020. Complete mitochondrial genomes of two deep-sea pandalid shrimps, *Heterocarpus ensifer* and *Bitias brevis*: insights into the phylogenetic position of Pandalidae (Decapoda: Caridea). *Journal of Oceanology and Limnology*, **38**: 816–825.

Sun, S.E., Hui, M., Wang, M. & Sha, Z. 2018. The complete mitochondrial genome of the alvinocaridid shrimp *Shinkaicaris leurokolos* (Decapoda, Caridea): Insight into the mitochondrial genetic basis of deep-sea hydrothermal vent adaptation in the shrimp. *Comparative Biochemistry and Physiology D*, **25**: 42–52.

Tamura, K., Stecher, G. & Kumar, S. 2021. MEGA11: molecular evolutionary genetics analysis version 11. *Molecular Biology and Evolution*, **38**: 3022–3027.

Tan, M.H., Gan, H.M., Schultz, M.B. & Austin, C.M. 2015. MitoPhAST, a new automated mitogenomic phylogeny tool in the post-genomic era with a case study of 89 decapod mitogenomes including eight new freshwater crayfish mitogenomes. *Molecular Phylogenetics and Evolution*, **85**: 180–188.

Triay-Portella, R., Ruiz-Díaz, R., Pajuelo, J.G. & González, J.A. 2017. Ovarian maturity, egg development, and offspring generation of the deep-water shrimp *Plesionika edwardsii* (Decapoda, Pandalidae) from three isolated populations in the eastern North Atlantic. *Marine Biology Research*, **13**: 174–187.

Tyagi, K., Chakraborty, R., Cameron, S.L., Sweet, A.D., Chandra, K. & Kumar, V. 2020. Rearrangement and evolution of mitochondrial genomes in Thysanoptera (Insecta). *Scientific Reports*, **10**: [https://doi.org/10.1038/s41598-020-57705-4].

Wang, Y., Zeng, L., Wen, J., Li, X., Huang, Y., Sun, Y. & Zhao, J. 2020. The complete mitochondrial genome of *Thor amboinensis* (Hippolytidae, Decapoda). *Mitochondrial DNA Part B*, **5**: 3077–3078.

Zhang, Z., Li, J., Zhao, X.Q., Wang, J., Wong, G.K.S. & Yu, J. 2006. KaKs_Calculator: calculating Ka and Ks through model selection and model averaging. *Genomics, Proteomics and Bioinformatics*, **4**: 259–263.

Zhu, L., Zhu, Z., Zhu, L., Wang, D., Wang, J. & Lin, Q. 2021. The complete mitogenome of *Lysmata vittata* (Crustacea: Decapoda: Hippolytidae) with implication of phylogenomics and population genetics. *PLoS ONE*, **16**: e0255547 [https://doi.org/10.1371/JOURNAL.PONE.0255547].